



HAL
open science

Photo and thermochemical evolution of astrophysical ice analogues as a source for soluble and insoluble organic materials in Solar system minor bodies

Pierre de Marcellus, Aurelien Fresneau, Rosario Brunetto, Grégoire Danger, Fabrice Duvernay, Cornelia Meinert, Uwe Meierhenrich, Ferenc Borondics, Thierry Chiavassa, Louis Le Sergeant D'hendecourt

► To cite this version:

Pierre de Marcellus, Aurelien Fresneau, Rosario Brunetto, Grégoire Danger, Fabrice Duvernay, et al.. Photo and thermochemical evolution of astrophysical ice analogues as a source for soluble and insoluble organic materials in Solar system minor bodies. Monthly Notices of the Royal Astronomical Society, 2017, 464 (1), pp.114 - 120. 10.1093/mnras/stw2292 . hal-01930506

HAL Id: hal-01930506

<https://hal.science/hal-01930506>

Submitted on 2 Aug 2022

HAL is a multi-disciplinary open access archive for the deposit and dissemination of scientific research documents, whether they are published or not. The documents may come from teaching and research institutions in France or abroad, or from public or private research centers.

L'archive ouverte pluridisciplinaire **HAL**, est destinée au dépôt et à la diffusion de documents scientifiques de niveau recherche, publiés ou non, émanant des établissements d'enseignement et de recherche français ou étrangers, des laboratoires publics ou privés.

Photo and thermochemical evolution of astrophysical ice analogues as a source for soluble and insoluble organic materials in Solar system minor bodies

Pierre de Marcellus,¹ Aurelien Fresneau,² Rosario Brunetto,¹ Gregoire Danger,^{2*} Fabrice Duvernay,² Cornelia Meinert,³ Uwe J. Meierhenrich,³ Ferenc Borondics,⁴ Thierry Chiavassa² and Louis Le Sergeant d’Hendecourt^{1*}

¹*Institut d’Astrophysique Spatiale, CNRS, Univ. Paris-Sud, Université Paris-Saclay, Bât. 121, F-91405 Orsay cedex, France*

²*Aix-Marseille Université, CNRS, PIIM UMR 7345, F-13397 Marseille, France*

³*Institut de Chimie de Nice, UMR 7272 CNRS, University Nice Sophia Antipolis, 28 Avenue Valrose, F-06108 Nice, France*

⁴*SMIS Beamline, Soleil Synchrotron, BP48, L’Orme des Merisiers, F-91192 Gif sur Yvette Cedex, France*

Accepted 2016 September 8. Received 2016 September 1; in original form 2016 June 18

ABSTRACT

Soluble and insoluble organic matter (IOM) is a key feature of primitive carbonaceous chondrites. We observe the formation of organic materials in the photothermochemical treatment of astrophysical ices in the laboratory. Starting from a low vacuum ultraviolet (VUV) irradiation dose on templates of astrophysical ices at 77 K, we obtain first a totally soluble form of organic matter at room temperature. Once this organic residue is formed, irradiating it further in vacuum results in the production of a thin altered dark crust on top of the initial soluble one. The whole residue is studied here by non-destructive methods inducing no alteration of samples, visible microscopy and mid-infrared (micro-)spectroscopy. After water extraction of the soluble part, an insoluble fraction remains on the sample holder which provides a largely different infrared spectrum when compared to the one of the soluble sample. Therefore, from the same VUV and thermal processing of initial simple ices, we produce first a soluble material from which a much larger irradiation dose leads to an insoluble one. Interestingly, this insoluble fraction shows some spectral similarities with natural samples of IOM extracted from two meteorites (Tagish Lake and Murchison), selected as examples of primitive materials. It suggests that the organic molecular diversity observed in meteorites may partly originate from the photo and thermal processing of interstellar/circum-stellar ices at the final stages of molecular cloud evolution towards the build-up of our Solar system.

Key words: astrochemistry – molecular processes.

1 INTRODUCTION

Organic matter is observed in many astrophysical environments, from the interstellar medium to our Solar system (Herbst & van Dishoeck 2009). It is present either as relatively simple molecules, observed by radio astronomy in the gas phase of molecular clouds (http://www.astrochymist.org/astrochymist_ism.html) and comets (Bockelée-Morvan et al. 2004), or much more complex solid-state (macro)molecular materials detected in interplanetary objects fallen on Earth, such as carbonaceous chondrites (Ehrenfreund & Charnley 2000; Schmitt-Kopplin et al. 2010).

One of the possible origins for this organic molecular complexity is the chemical evolution of solid interstellar/circum-stellar ices. Indeed, the solid-state nature of the bulk of simple ices offers favourable conditions to obtain a wide molecular diversity as observed in laboratory experiments (Danger et al. 2013) and favourably compared with the one observed in meteorites (Danger et al. 2016). Ices are formed by the condensation of volatile compounds onto the surface of silicate (or carbon) grains in dense molecular clouds and protoplanetary discs. They are widely observed, in the mid-infrared (IR) spectral range, in regions of star formation and are mostly composed of water, one of the most abundant gas phase molecule besides H₂, followed by CO, CO₂, CH₃OH, NH₃, CH₄, etc. (Öberg et al. 2011). In these environments, they are exposed to different energetic processes, such as cosmic rays, vacuum ultraviolet (VUV) photons and/or heating. Under these processes,

* E-mail: gregoire.danger@univ-amu.fr (GD); ldh@ias.u-psud.fr (LLSd’H)

an intricate solid-state chemistry occurs, leading to the formation of new and (much) more complex molecules, often more refractory than simple ices, some of which are observed in the gas phase of hot molecular cores (Belloche et al. 2013) with abundances that cannot be explained by gas phase reactions alone (Garrod, Widicus Weaver & Herbst 2008).

In the laboratory, experiments simulating the photothermochemical evolution of cosmic ices are routinely performed. These simulations have shown that, after warming up irradiated ice samples to room temperature, a semirefractory organic residue is always formed (Agarwal et al. 1985; Briggs et al. 1992). These residues are composed of organic macromolecules (Danger et al. 2013, 2016) mixed with individual species (Muñoz Caro et al. 2002; de Marcellus et al. 2011, 2015; Meinert et al. 2012, 2016), and are considered as analogues of pre-cometary organic matter that may have played some role in prebiotic chemistry if delivered to a telluric planet such as the Earth (Oro 1961; de Marcellus et al. 2015). In our series of experiments, the residues are totally soluble in polar solvents like water or methanol and can then be compared with the soluble organic matter (SOM) of primitive chondrites that constitutes up to 30 per cent of their organic content (Sephton 2002; Martins et al. 2015). The rest of the meteoritic organic matter is insoluble and usually known as insoluble organic matter (IOM; Derenne & Robert 2010). The source of both meteoritic SOM and IOM is a long debated issue and remains poorly understood (Hayatsu et al. 1977; Cronin & Chang 1993; Alexander et al. 1998, 2007; Cody et al. 2011; Quirico et al. 2014). Although the origin and further evolution of this organic matter is difficult to fully apprehend and certainly non-univocal, photo and thermochemical processes on simple and abundant ices, at the pre-accretional stage and later on in protoplanetary discs (Ciesla & Sandford 2012) may account for at least a significant part of its formation.

In this work, we have produced laboratory organic residues from photo/thermo-chemistry of astrophysical ices analogues to investigate the possibility to form insoluble organic materials from soluble organic ones. The samples were monitored by IR vibrational spectroscopy and the IR spectra of our insoluble residue were related to IR spectra of IOM extracted from two primitive carbonaceous meteorites, Tagish Lake and Murchison. Similarities in the spectra are indeed observed and discussed in terms of a possible evolutionary link between these two materials.

2 METHODS

Our experimental setup has been described in detail elsewhere (Nuevo et al. 2007). In brief, it consists of a vacuum chamber pumped down to 10^{-7} mbar, in which a substrate (here a zinc-selenium, ZnSe, window) is cooled down to 77 K, thanks to an open cycle liquid-N₂ cryostat. A gas mixture is prepared in a separate stainless steel line, previously pumped down to 10^{-6} mbar. It is then injected into the vacuum chamber where it condenses onto the substrate to form a film of interstellar ice analogue. Simultaneously to the deposition, the ice mixture is irradiated by VUV photons generated by an H₂ discharge lamp (Chen et al. 2014). The experiment is monitored by *in situ* Fourier transform infrared transmission spectroscopy. This classical technique allows for a direct and global comparison at the macroscopic scale, with astronomical data and/or extraterrestrial samples as a first insight into the relevance of the performed laboratory simulations (D’Hendecourt et al. 1996; d’Hendecourt & Dartois 2001). In addition, IR spectra of the deposited mixture are used to monitor the deposition rate and relative abundances of the molecules in the initial ice.

Two samples were produced independently from the same ice mixture, H₂O:CH₃OH:NH₃ = 3:1:1, qualitatively representative of interstellar/circum-stellar ices. The first step consists of depositing the gas mixture onto the cold window for 90 (sample 1) and 15 (sample 2) h, respectively. Both deposits are performed with simultaneous VUV irradiation to ensure a homogeneous irradiation in the bulk of the sample, representing an ~ 10 eV VUV energy dose per deposited molecule. The deposition rate is around 10^{14} molecules cm⁻² s⁻¹. Subsequent warm up (~ 0.1 K min⁻¹) to room temperature is then performed by switching off the coolant supply. During this step, all the volatile species from either the initial ice or the main photoproducts (e.g. CO, CO₂...) progressively sublime. Radicals and reactants diffuse and recombine to form complex and more refractory species that remain on the substrate at room temperature. During this process, a rather large part of the initial material was lost (Muñoz Caro & Schutte 2003). At room temperature (295 K), we obtain two organic residues of different thicknesses. Both residues are subsequently VUV irradiated in vacuum for 73 h. The penetration depth of the VUV photons in the organic residues is only a few tens of nanometres (Bennett, Pirim & Orlando 2013). The total dose is now estimated to lie in the range of a few tens of keV per bond as an order of magnitude (calculated for a UV penetration depth of ~ 50 nm, assuming an average density of 2 for the organic residue and a photon flux of 10^{14} cm⁻² s⁻¹, characteristic of the VUV lamp used here). Note that this dose represents now roughly a factor of a few thousands more energy per bond than the one delivered on the initial simple ices sample. At the end of this second irradiation, the remaining SOM of both samples is extracted in water by soaking the ZnSe windows in Milli-Q water for 14 h at room temperature. They are subsequently dried in a desiccator for 45 min under dynamic oil-free pumping. The production of the insoluble fraction is schematically depicted in Fig. 1, right-hand panel.

Some of the spectroscopic analyses of sample 1 were made *ex situ*, on the SMIS (Spectroscopy and Microscopy in the IR using Synchrotron) beamline (Dumas et al. 2006) of the SOLEIL synchrotron (Gif-sur-Yvette, France). The ZnSe window was removed from the vacuum chamber, and transferred to the analytical instrument in an individual stainless steel sample holder under argon atmosphere to minimize possible chemical effects from oxygen or residual moisture from the atmosphere. IR micro-analysis was performed using NicPlan and Continuum XL microscopes, coupled to NEXUS 6700 FTIR spectrometers (Thermo Fisher). The measurements were carried out in transmission geometry through the ZnSe window. During the process, samples were exposed to air for several hours. IR beam spots ranging from ~ 10 to ~ 100 μ m on the samples (32X objective) were used. We collected spectra in the mid-IR (5000–650 cm⁻¹ or 2–15.4 μ m) using an MCT detector with a spectral resolution of 2 cm⁻¹.

3 RESULTS

A mosaic picture of sample 1 can be seen in Fig. 1, left-hand panel. Contrary to what can be expected, the sample (Fig. 1a) is not spatially homogeneous. The central part of the sample has been lost during the warming step, possibly because of exothermic radical-radical recombinations that may account for explosive sublimation (d’Hendecourt et al. 1982; Rawlings et al. 2013). The organic residue is characterized by thin homogeneous as well as thicker (and darker) areas, droplet-shaped structures already mentioned by (Dworkin et al. 2001). The overirradiation step has induced a dramatic change of the sample’s visual appearance (Fig. 1b). Its surface is now much darker and shows a varnish aspect with a dark

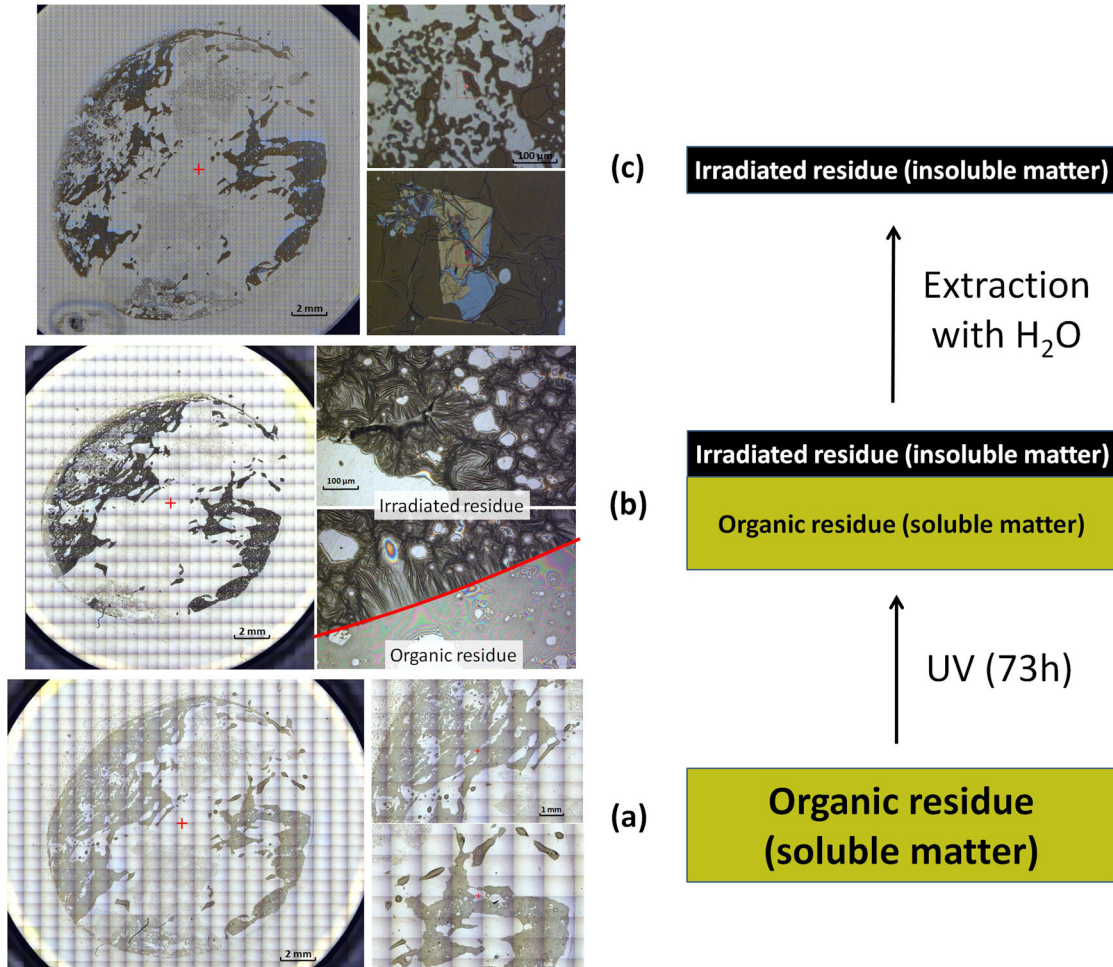


Figure 1. Visible light Microscope pictures of sample 1 (left), schematically portrayed at different stages of its evolution (right). (a) Initial non-photolyzed organic residue at room temperature, exclusively composed of soluble material. (b) After 73 h of VUV irradiation in vacuum, forming a thin crust of insoluble material. A small part was not overirradiated and the difference is marked by the red separation line. (c) After removing the soluble part with liquid water, only the insoluble material remains here on the window.

micro-layered surface. It should be noted here that the edge of the residue was not irradiated and kept its initial nature, which allows a direct visual comparison with the over-irradiated matter.

Fig. 2(a) shows an IR spectrum at the macro-scale in the cryostat of this non-irradiated residue (sample 1), thus only containing the SOM. Considering our experimental conditions, this is a typical spectrum, which displays features of individual molecules such as hexamethylenetetramine (HMT) with bands located mainly at 1005, 1235, 1366 and 1461 cm^{-1} (Bernstein et al. 1995; Vinogradoff et al. 2011; Briani et al. 2013) as well as several overlapping bands that can be attributed to alcohols, carboxylic acids, amines, amides, esters, etc. (Bernstein et al. 1995; Muñoz Caro & Schutte 2003).

The IR spectrum corresponding to the irradiated residue is displayed in Fig. 2(b). Compared to spectrum 2a, the absorbance has slightly decreased for most of the bands, in particular, the $\text{C}=\text{O}$ stretching band at 1750 cm^{-1} , but a band at 2150 cm^{-1} has grown, which can be attributed to an isocyanate function ($\text{R}-\text{N}=\text{C}=\text{O}$) (Brucato, Baratta & Strazzulla 2006). In spite of these small differences, the two spectra are overall similar. The fact that the visible pictures (1a and b) display such a striking difference in appearance when the corresponding IR spectra (2a and b) show large similarities can be explained by the penetration depth of VUV photons, which is much smaller than the organic residue's thickness (a few

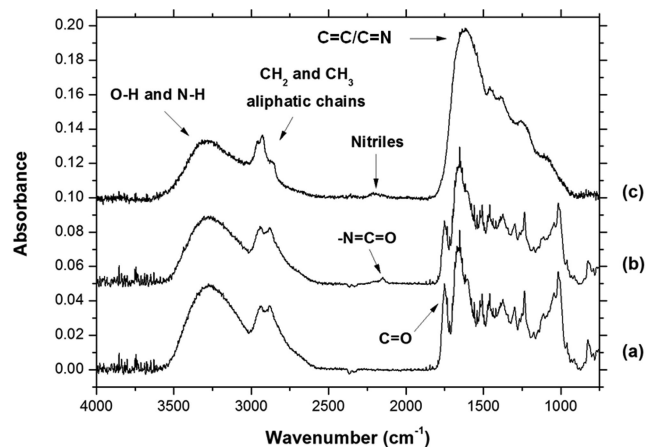


Figure 2. Infrared spectra of sample 1, corresponding to Fig. 1 sequence. (a) Non-irradiated organic residue. (b) VUV-irradiated residue (73 h). (c) Insoluble matter only, after liquid water extraction. Spectra (a) and (b) were taken *in situ* in the vacuum of the cryogenic chamber. Spectrum (c) was obtained using the IR microscope at the SOLEIL synchrotron SMIS beamline.

tens of nanometers for the VUV penetration depth as opposed to a few micrometres for the thickest areas of the final sample). Irradiation has thus transformed only the first top layers of the organic residue, forming a thin crust of overphotolyzed matter. The optical microscope analysis provides a picture of the sample surface, which clearly shows a morphology variation after overirradiation.

On the other hand, the IR beam probes the full depth of the sample, leading to an average spectrum of the whole material. The IR transmission spectrum remains thus still largely dominated by the non-photolyzed residue. We assume that, owing to the observed morphological changes, the top layers have been transformed from soluble to insoluble material. To test this hypothesis, the sample was then washed with water to remove the soluble organic part and dried, as described in the experimental section.

An image of the resulting sample is visible in Fig. 1(c) where the soluble part has been removed. Except for the non-photolyzed parts (soluble material), all the structures are still present, showing that an insoluble material has indeed been formed as a crust where the residue was overirradiated. Coloured structures (right, bottom) are actually composed of the same material, but thicker, thus scattering differently the visible light from the microscope. Fig. 2(c) presents the IR spectrum of one of the thickest areas of this insoluble component, here obtained with the IR microscope (spot size 25 μm), whereas spectra 2a and 2b were obtained within the cryostat, representing an average spectrum of the whole sample. It should be noted that the presence and the relative ratios of the bands in spectrum 2c are identical throughout the sample, independently of the position of the IR beam of the microscope. This last spectrum pertaining to the insoluble material will now be discussed in more detail. Bands identifications were made following Bellamy (1975) and Socrates tables (Bellamy 1975; Socrates 2004).

Compared to the soluble material, the bands related to HMT have totally disappeared. Furthermore, in the range of 1800–900 cm^{-1} , the spectrum appears simpler with a few noticeable broad bands. Features at 1457 and 1385 cm^{-1} can be attributed to asymmetric and symmetric wagging modes of aliphatic $-\text{CH}$ ($-\text{CH}_3$). Another broad feature centred on 1240 cm^{-1} can be related to aromatic skeletal modes (Ferrari, Rodil & Robertson 2003). A stretching C–O band is seen at 1097 cm^{-1} . Finally, the most prominent feature appears at 1616 cm^{-1} which contains several contributions (see Fig. 3A). The following weak carbonyl bands ($\nu\text{C}=\text{O}$) are tentatively observed at 1770 cm^{-1} for esters, 1713 cm^{-1} for carbonyls on aliphatic structures, and 1680 cm^{-1} for amides. Finally several bands are also present between 1616 and 1585 cm^{-1} that can be related to $\text{C}=\text{C}$ (alkenes or aromatics) or imines ($\text{C}=\text{N}$) stretching modes. In the higher frequency range (Fig. 3B), a broad band centred at 3350 cm^{-1} is attributed to O–H and N–H stretching modes (alcohols, carboxylic acids and/or amines). Finally, a nitrile $\text{C}\equiv\text{N}$ band is also observed at 2200 cm^{-1} . Several well-known features of aliphatic C–H stretching modes are present around 2950 cm^{-1} and, next to it, a quite small contribution of $\text{sp}^2 = \text{C}-\text{H}$ stretch (alkenes or aromatics) is detected. Basically, this new material presents a more unsaturated carbon backbone than the initial non-overirradiated soluble organic residue, with a few heteroatoms functions.

In order to confirm that the spectral changes were actually only due to the VUV irradiation, a second sample (thinner) was prepared. A macro IR spectrum (in the cryostat) of sample 2, before overirradiation, is shown in Fig. 4(a), and presents the characteristic features of soluble organic residues. It is similar to the IR spectrum of sample 1 (Fig. 2a) except for the HMT bands, which are stronger, and the O–H bands at 3280 and 1670 cm^{-1} , which are weaker. Sample 1 was exposed to air for micro-scale analyses, and macro-scale

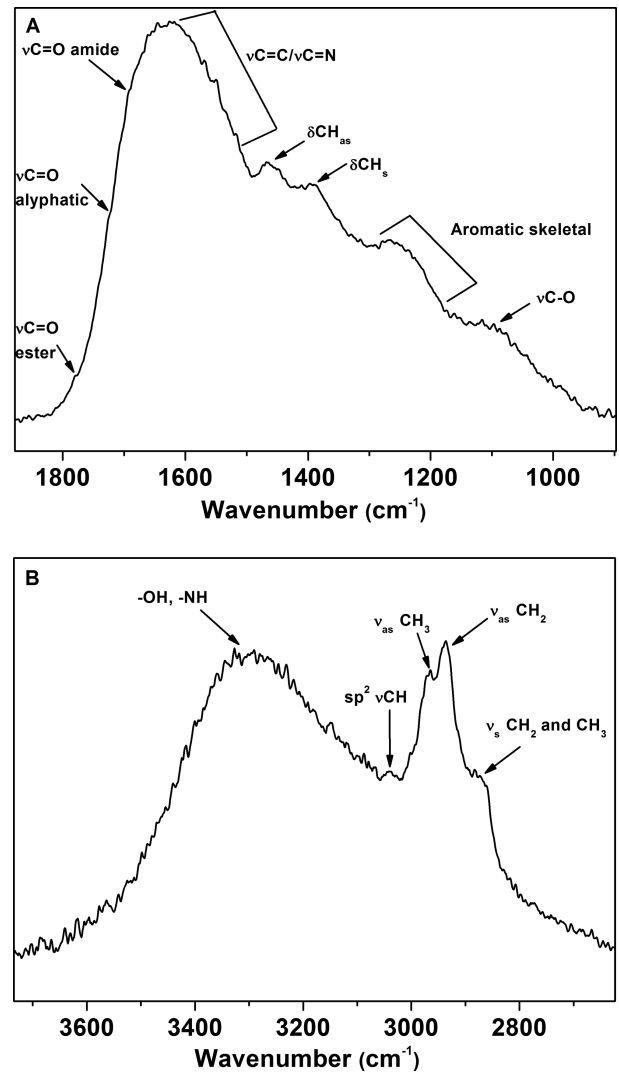


Figure 3. Enlarged version of the infrared spectrum of the insoluble fraction of the overirradiated residue (2c) in the 3700–2700 cm^{-1} region of the spectrum (A) and in the region 1800–900 cm^{-1} (B). See Table 1 for a comparison with Tagish Lake features.

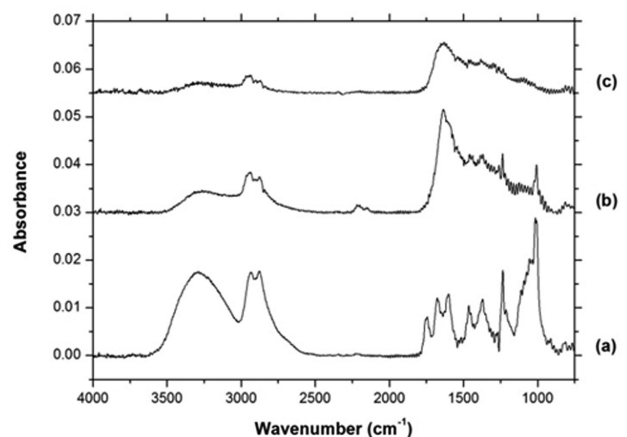


Figure 4. Infrared spectra of sample 2. (a) Non-irradiated organic residue, much thinner than sample 1. (b) VUV-irradiated (73 h) residue. (c) Photolyzed (insoluble) matter only, after liquid water extraction. The spectra were all taken within the cryogenic chamber.

IR spectroscopy was then performed after this exposure, explaining these differences.

These differences are due to the exposure to air of sample 1 during the micro-IR analyses that lasted ~ 30 h, resulting in the loss of some HMT, which is volatile at room temperature, and the adsorption of some atmospheric water. Since this sample 2 was much thinner than sample 1, a much larger fraction of this second organic residue was photolyzed. As opposed to sample 1, spectra before (4a) and after overirradiation (4b) of sample 2 now do show a clear change that tends to resemble the insoluble material spectrum just described above 2c. However, the sample was still optically thick to VUV radiation and the soluble part was not totally converted into IOM through photolysis since HMT features are still present. Fig. 4(c) finally displays the macro IR spectrum of sample 2 after water extraction of the soluble part. This spectrum is now almost identical to the one obtained for sample 1 (2c). This comparison between micro- (Fig. 2c) and macro-scales (Fig. 4c) IR spectrum clearly demonstrates that once the insoluble material is formed and washed off the soluble material, the insoluble part is homogeneously distributed across the sample. The insoluble part lies actually on top of the soluble one prior to water extraction on both samples.

As a conclusion of our results, we consider that spectrum 2c (sample 1) does represent a typical IR spectrum of an overirradiated organic residue. Our results demonstrate that it is indeed possible to form an insoluble organic material from a soluble organic one submitted to a subsequent VUV irradiation. This insoluble material then protects the soluble part from further VUV irradiation. Similar results were obtained by other groups using ion bombardment (Brucato, Baratta & Strazzulla 2006), although UV photons are thought to dominate the polymerization and carbonization process (Jenniskens et al. 1993).

4 ASTROPHYSICAL IMPLICATION

Our experimental approach is related to the late stages of the molecular cloud out of which the sun, planets and many debris formed. Icy grains were exposed to various irradiation and thermal heating effects during the formation of the solar nebula as well as most probably during the protoplanetary disc early evolution, as depicted in the model of Ciesla & Sandford (2012). As shown from our laboratory experiments, some soluble and insoluble organic materials

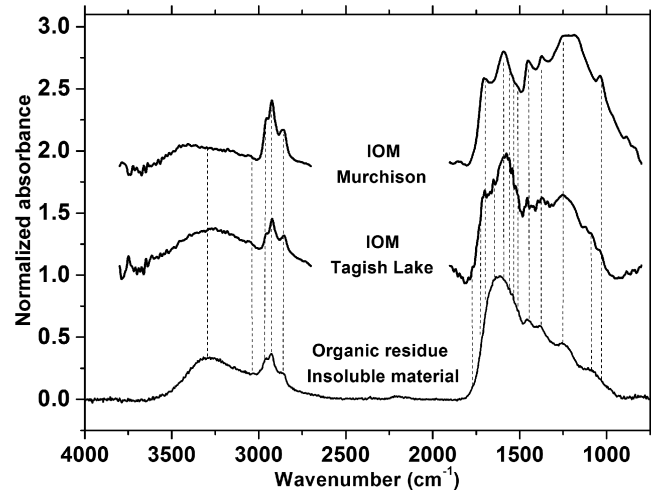


Figure 5. Comparison between the infrared spectra of our insoluble residue (bottom) with the spectra of IOM extracted from Tagish Lake and Murchison. For meteorites, data are taken from Kebukawa et al. (2011). The vertical dotted lines refer to the bands observed in the enlarged figure from the infrared spectrum of the residue (Figs 3A and B).

can find their origin in the photo and thermal evolution of ices. The icy grains then agglomerated during the accretion phase and were incorporated into planetesimals whose leftovers are minor bodies such as asteroids and comets, the parent bodies of meteorites.

In Fig. 5, we associate the IR spectrum of our produced insoluble material with the spectra of IOM extracted from two most primitive and organic carbon rich chondrites, Tagish Lake and Murchison, for which data are available in the literature. The insoluble material obtained from our template of interstellar ices shows a noticeable IR spectral resemblance with the IOM of the Tagish Lake meteorite (data from Kebukawa, Alexander & Cody 2011) in terms of band positions (Table 1). Among the 15 IR bands identified in our residue, 14 band positions correspond to those observed in the IOM of Tagish Lake. Thus, similar chemical functions are present in both insoluble materials produced from simple ices and the Tagish Lake IOM. Some differences are, however, visible in band intensities and bandwidths. Therefore, the chemical structures of these two samples are different while presenting similar chemical functions.

Table 1. Comparison between the observed features in the overirradiated laboratory residue and the main features appearing in the IOM extracted from Tagish Lake (IOM data from Kebukawa et al. 2011).

Peak position (cm^{-1})		Vibrational mode	Functional group
Insoluble material	IOM Tagish lake		
3326	3400	O–H stretch	Alcohol, carboxyl
3030	3060	C–H stretch	Aromatic CH
2956	2955	C–H asymmetric stretch	Aliphatic CH_3
2926	2925	C–H asymmetric stretch	Aliphatic CH_2
2872	2870	C–H symmetric stretch	Aliphatic CH_3
2855	2855	C–H symmetric stretch	Aliphatic CH_2
2200	nd	$\text{C}\equiv\text{N}$ stretch	nitrile
1729	1725	C=O stretch	Esters
1713	1710	C=O stretch	Aliphatic ketones
1682	1665	C=O stretch	Amide
1616–1585	1600–1580	C=C or C=N stretch	Alkene, Imine, Aromatic
1457	1455	C–H asymmetric bend	Aliphatic CH_3
1385	1375	C–H symmetric bend	Aliphatic CH_3
1240	1210	Aromatic skeletal	
1097	1160	C–O stretch	

Especially, the band related to the aromatic skeletal vibration (1240 cm^{-1}) in Tagish Lake is clearly wider and much more intense than in our insoluble material suggesting a higher degree of maturation of the organic matter of Tagish Lake and thus a far more developed sp^2 carbon network (Carpentier et al. 2012), more similar to a kerogen. The IR spectral differences are somewhat more important with the Murchison meteorite, in particular, the $\text{C}=\text{O}$ band at 1710 cm^{-1} and the aromatic skeleton vibrational modes around 1240 cm^{-1} which shows an even larger intensity. For the carbonyl stretch, we note that this band has disappeared upon overirradiation in our samples. As it is present in meteoritic IOM, it might find its origin in the post-accretion evolution of the planetesimals where oxidative processes (via aqueous alteration and/or thermal metamorphism) were at work (see Kebukawa et al. 2011 and references therein; Kebukawa et al. 2011).

Our insoluble organic material produced in the laboratory is thus only a step toward meteoritic IOM and would require additional processes to improve the match, such as thermal metamorphism, aqueous alteration or the possible interactions with the various mineral phases usually present in parent bodies of meteorites. Incidentally, Raman analyses at 532 nm of our samples did not show any *D* and *G* bands but only a high level of fluorescence, already noticed by (Muñoz-Caro et al. 2006). This absence likely results from a far lesser maturation and organization of the carbon structural units in our samples as compared to meteorites, a well-known phenomenon described for instance in Marchand (1986) to explain the onset of graphitization in amorphous carbon materials.

It should be noted, as clearly shown in the original data from Kebukawa, Alexander & Cody (2011), that each meteorite presents its own IR spectrum and thus meteoritic IOM cannot be characterized by a unique spectrum. This reflects a natural tendency to heterogeneity that is observed within different classes of meteorites as well as within the same meteorite. These heterogeneities are due to specific and local evolution of this matter upon different conditions.

The origin of IOM in primitive meteorites is a longstanding and debated problem (Quirico et al. 2014). Despite its importance as a tracer for different physical processes in the solar nebula, one should keep in mind that this IOM is always mixed, although in different proportions, with the SOM, which represents from 5 to 30 per cent in mass of the organic matter within different classes of meteorites (Sephton 2002). Our laboratory results clearly indicate that the evolution from soluble to insoluble material is possible as a consequence of further UV irradiation of the soluble material originating from ices. This result is also well supported by the observation of organic globules in Tagish Lake by Nakamura-Messenger et al. (2006). These globules, revealing a high *D/H* ratio, are thought to be compatible with the organic residues produced from ices photochemistry in cold environments. In poorly altered meteorites like those just cited before, as well as in the Paris meteorite, a pristine fraction of the SOM and IOM originating from the photochemistry of astrophysical ices may well have been preserved in the matrix of the meteorite. This hypothesis is supported by the recent *in situ* analyses of the organic matter distribution inside meteorites by Le Guillou (Le Guillou & Brearley 2014; Le Guillou et al. 2014), which indicates that some soluble and insoluble materials can be brought together with water during the grain accretion forming the meteorite parent bodies. Indeed, as tentatively shown in Merouane et al. (2012), micro-IR spectral similarities between some selected carbon-rich fragments from the Paris meteorite matrix and some features observed towards a molecular cloud IR source (GCS3)

have been reported. It suggests the likely presence of some interstellar hydrocarbons in Paris and thus a genuinely unaltered fraction of organic matter in this meteorite, which suffered quite a small degree of aqueous alteration as discussed by Hewins et al. (2014) and, especially from the molecular carbon distribution, also pointed out by Martins et al. (2015).

Other sources of insoluble material, involving experimental simulations of hot plasma condensation in the internal solar nebula have recently been proposed (Biron et al. 2015; Kuga et al. 2015). These experiments may indeed account for a more mature insoluble material production but without explaining the formation of the soluble oxygen-rich material that is also included in primitive meteorites. In this case, the formation of this IOM would require a mechanism within the inner solar nebula but both mechanisms may well co-exist in the building up of the meteoritic IOM. As for our hypothesis involving ices, we may also note that radial mixing from turbulent motions of materials from different origins, in particular, from cold ices towards the inside of the Solar system, has been proposed for example by Bockelée-Morvan et al. (2002). Certainly, the origin of organic matter in meteorites is not univocal and should come from different processes.

5 CONCLUSIONS

From simple molecular ices (H_2O , CH_3OH and NH_3) and UV photons only, we form a complex soluble organic material (the organic residue). Upon excess irradiation, an insoluble fraction is formed. A noticeable similarity in the IR spectra with Tagish Lake IOM is observed and, to a lesser extent, with Murchison IOM.

Empirically, we propose a mechanism that would explain the presence, at least in part, of both soluble and insoluble material in astrophysical objects. The soluble fraction formation occurs from the photo and thermal processing (or radiolysis) of astrophysical ices during the solar nebula formation and its subsequent evolution into a protoplanetary disc. This soluble material becomes progressively more and more photo and/or ion-processed at the surface of the grains forming an insoluble crust. This crust protects the underlying soluble fraction from further UV irradiation and thus from photodestruction. During the accretion, both soluble and insoluble materials are incorporated into planetesimals of the Solar system, some of which are parent bodies of meteorites. These organics can evolve in these minor bodies of different sizes, following various possible secondary alteration pathways such as thermal metamorphism and/or aqueous alteration, and are finally converted into the organic materials found in carbonaceous meteorites SOM and IOM, although some may have remained preserved from further processing as suggested by the very low alteration phases observed in some meteorites. Only further laboratory studies taking into account these secondary alteration processes may help to produce more mature materials approaching meteoritic organic matter and to propose a global astrophysical scenario for its origin.

ACKNOWLEDGEMENTS

We are indebted to Dr Y. Kebukawa for providing the Tagish Lake and Murchison IOM electronic data. This experiment is part of the MICMOC set-up financed by the Centre National d'Etudes Spatiales (CNES). This work has been also funded by French national programmes 'Programme National de Planétologie' (PNP, INSU), 'Programme de Physique et Chimie du Milieu Interstellaire' (PCMI, INSU) and the 'CNES' from its exobiology programme.

REFERENCES

- Agarwal V. K., Schutte W., Greenberg J. M., Ferris J. P., Briggs R., Connor S., van de Bult C. P. E. M., Baas F., 1985, *Orig. Life Evol. Biosph.*, 16, 21
- Alexander C. M. O., Russell S. S., Arden J. W., Ash R. D., Grady M. M., Pillinger C. T., 1998, *Meteorit. Planet. Sci.*, 33, 603
- Alexander C. M. O., Fogel M. L., Yabuta H., Cody G. D., 2007, *Geochem. Cosmol. Acta*, 71, 4380
- Bellamy L. J., 1975, *The Infrared Spectra of Complex Molecules*. Wiley, New York
- Belloche A., Müller H. S. P., Menten K. M., Schilke P., Comito C., 2013, *Astron. Astrophys.*, 559, A47
- Bennett C. J., Pirim C., Orlando T. M., 2013, *Chem. Rev.*, 113, 9086
- Bernstein D. I., Sandford S. A., Allamandola L. J., Chang S., Bernstein M., Scharberg M. A., 1995, *ApJ*, 454, 327
- Biron K., Derenne S., Robert F., Rouzaud J. N., 2015, *Meteorit. Planet. Sci.*, 50, 1408
- Bockelée-Morvan D., Gautier D., Hersant F., Huré J.-M., Robert F., 2002, *A&A*, 384, 1107
- Bockelée-Morvan D., Crovisier J., Mumma M. J., Weaver H. A., 2004, in Festou M., Keller H. U., Weaver H. A., eds, *Comets II*. Univ. Arizona Press, Tuscan, AZ, p. 391
- Briani G., Fray N., Cottin H., Benilan Y., Gazeau M.-C., Perrier S., 2013, *Icarus*, 226, 541
- Briggs R., Ertem G., Ferris J. P., Greenberg J. M., McCain P. J., Mendoza-Gomez C. X., Schutte W., 1992, *Orig. Life Evol. Biosph.*, 22, 287
- Brucato J. R., Baratta G. A., Strazzulla G., 2006, *A&A*, 455, 395
- Carpentier Y. et al., 2012, *A&A*, 548, A40
- Chen Y.-J. et al., 2014, *ApJ*, 781, 15
- Ciesla F. J., Sandford S. A., 2012, *Science*, 336, 452
- Cody G. D., Heying E., Alexander C. M. O., Nittler L. R., Kilcoyne A. L. D., Sandford S. A., Stroud R. M., 2011, *Proc. Natl. Acad. Sci. USA*, 108, 19171
- Cronin J. R., Chang S., 1993, in Greenberg J. M. et al., eds, *Organic Matter in Meteorites: Molecular and Isotopic Analyses of the Murchison Meteorite, The Chemistry of Life's Origins*. Springer, the Netherlands, p. 209
- d'Hendecourt L., Dartois E., 2001, *Spectrochim. Acta A*, 57, 669
- D'Hendecourt L. B., Allamandola L. J., Baas F., Greenberg J. M., 1982, *A&A*, 109, L12
- D'Hendecourt L. L. S. et al., 1996, *A&A*, 315, L365
- Danger G. et al., 2013, *Geochim. Cosmochim. Acta*, 118, 184
- Danger G. et al., 2016, *Geochim. Cosmochim. Acta*, 189, 184
- de Marcellus P. et al., 2011, *ApJ*, 727, L27
- de Marcellus P., Meinert C., Myrgorodska I., Nahon L., Buhse T., d'Hendecourt L. L. S., Meierhenrich U. J., 2015, *Proc. Natl. Acad. Sci.*, 112, 965
- Derenne S., Robert F., 2010, *Meteorit. Planet. Sci.*, 45, 1461
- Dumas P., Polack F., Lagarde B., Chubar O., Giorgetta J. L., Lefrançois S., 2006, *Infrared Phys. Technol.*, 49, 152
- Dworkin J. P., Deamer D. W., Sandford S. A., Allamandola L. J., 2001, *Proc. Natl. Acad. Sci. USA*, 98, 815
- Ehrenfreund P., Charnley S. B., 2000, *Annu. Rev. Astron. Astr.*, 38, 427
- Ferrari A. C., Rodil S. E., Robertson J., 2003, *Phys. Rev. B*, 67, 155306
- Garrod R. T., Widicus Weaver S. L., Herbst E., 2008, *Astrophys. J.*, 682, 283
- Hayatsu R., Matsuoka S., Scott R. G., Studier M. H., Anders E., 1977, *Geochim. Cosmochim. Acta*, 41, 1325
- Herbst E., van Dishoeck E. F., 2009, *ARA&A*, 47, 427
- Hewins R. H. et al., 2014, *Geochim. Cosmochim. Acta*, 124, 190
- Jenniskens P., Baratta G. A., Kouchi A., de Groot M. S., Greenberg J. M., Strazzulla G., 1993, *A&A*, 273, 583
- Kebukawa Y., Alexander C. M. O. D., Cody G. D., 2011, *Geochim. Cosmochim. Acta*, 75, 3530
- Kuga M., Marty B., Marrocchi Y., Tissandier L., 2015, *Proc. Natl. Acad. Sci.*, 112, 7129
- Le Guillou C., Bernard S., Brearley A. J., Remusat L., 2014, *Geochim. Cosmochim. Acta*, 131, 368
- Le Guillou C., Brearley A., 2014, *Geochim. Cosmochim. Acta*, 131, 344
- Marchand A., 1986, in Léger A., d'Hendecourt L., Boccarda N., eds, *Poly-cyclic Aromatic Hydrocarbons and Astrophysics*. D. Reidel Publishing Company, Dordrecht, p. 31
- Martins Z., Modica P., Zanda B., d'Hendecourt L. L. S., 2015, *Meteorit. Planet. Sci.*, 50, 926
- Meinert C., Filippi J. J., de Marcellus P., Le Sergeant d'Hendecourt L., Meierhenrich U. J., 2012, *Chem. Plus Chem.*, 77, 186
- Meinert C., Myrgorodska I., de Marcellus P., Buhse T., Nahon L., Hoffmann S. V., d'Hendecourt L. L. S., Meierhenrich U. J., 2016, *Science*, 352, 208
- Merouane S., Djouadi Z., d'Hendecourt L. L. S., Zanda B., Borg J., 2012, *ApJ*, 756, 154
- Muñoz Caro G. M. et al., 2002, *Nature*, 416, 403
- Muñoz Caro G. M., Schutte W. A., 2003, *A&A*, 412, 121
- Muñoz-Caro G. M. et al., 2006, *A&A*, 459, 147
- Nakamura-Messenger K., Messenger S., Keller L. P., Clemett S. J., Zolensky M. E., 2006, *Science*, 314, 1439
- Nuevo M. et al., 2007, *Adv. Space Res.*, 39, 400
- Öberg K. I., Boogert A. C. A., Pontoppidan K. M., van den Broek S., van Dishoeck E. F., Bottinelli S., Blake G. A., Evans N. J., II, 2011, *ApJ*, 740, 109
- Oro J., 1961, *Nature*, 190, 389
- Quirico E. et al., 2014, *Geochim. Cosmochim. Acta*, 136, 80
- Rawlings J. M. C., Williams D. A., Viti S., Duley W. W., 2013, *MNRAS*, 430, 264
- Schmitt-Kopplin P. et al., 2010, *Proc. Natl. Acad. Sci.*, 107, 2763
- Sephton M., 2002, *Nat. Prod. Rep.*, 19, 292
- Socrates G., 2004, *Infrared and Raman Characteristic Group Frequencies, Tables and Charts*, 3rd edn. John Wiley & Sons Ltd, England
- Vinogradoff V., Duvernay F., Danger G., Theule P., Chiavassa T., 2011, *A&A*, 530, A128

This paper has been typeset from a $\text{\TeX}/\text{\LaTeX}$ file prepared by the author.